

Surface Decoration on Polymeric Gate Dielectrics for Flexible Organic Field-Effect Transistors via Hydroxylation and Subsequent Monolayer Self-Assembly

Yan Yan,[†] Long-Biao Huang,[†] Ye Zhou,[‡] Su-Ting Han,[†] Li Zhou,[†] Qijun Sun,[†] Jiaqing Zhuang,[†] Haiyan Peng,^{†,§} He Yan,^{||} and V. A. L. Roy^{*,†}

[†]Department of Physics and Materials Science, City University of Hong Kong, Tat Chee Avenue, Kowloon, Hong Kong SAR

[‡]Institute for Advanced Study, Shenzhen University, Shenzhen, Guangdong 508060, People's Republic of China

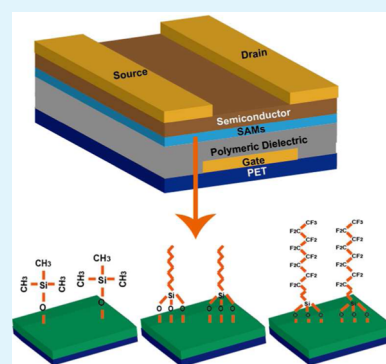
[§]Guangzhou Institute of Advanced Technology, Chinese Academy of Sciences, Guangzhou 511458, People's Republic of China

^{||}Department of Chemistry, Hong Kong University of Science and Technology, Clear Water Bay, Kowloon, Hong Kong

S Supporting Information

ABSTRACT: A simple photochemical reaction based on confined photocatalytic oxidation (CPO) treatment and hydrolysis was employed to efficiently convert C–H bonds into C–OH groups on polymeric material surfaces, followed by investigation of monolayer self-assembly decoration on polymeric dielectrics via chemical bonding for the organic field-effect transistors (OFETs) applications. This method is a low temperature process and has negligible etching effect on polymeric dielectric layers. Various types of self-assembled monolayers have been tested and successfully attached onto the hydroxylated polymeric dielectric surfaces through chemical bonding, ensuring the stability of decorated functional films during the subsequent device fabrication consisting of solution processing of the polymer active layer. With the surface decoration of functional groups, both n-type and p-type polymers exhibit enhanced carrier mobilities in the unipolar OFETs. In addition, enhanced and balanced mobilities are obtained in the ambipolar OFETs with the blend of polymer semiconductors. The anchored self-assembled monolayers on the dielectric surfaces dramatically preclude the solvent effect, thus enabling an improvement of carrier mobility up to 2 orders of magnitude. Our study opens a way of targeted modifications of polymeric surfaces and related applications in organic electronics.

KEYWORDS: field-effect transistors, hydroxylation, solution process, SAMs, ambipolar



INTRODUCTION

Organic field-effect transistors (OFETs), which have numerous applications in organic electronics such as price tags, “smart” cards, radio frequency identification tags (RFID), and back-plane circuitry for active matrix displays and sensors, are highly desirable for manufacturing large-area devices with high performance at low cost.^{1–11} Toward this end, extensive research efforts have been given. One of the vigorous investigations is through interface engineering, especially on the interface between the semiconductor and gate dielectric, since the semiconductor/dielectric interface has a significant impact on the morphology of the semiconductor that eventually determines overall electrical performances of devices. It is clear that the modification of a gate dielectric layer can achieve an improvement of OFETs’ performances.^{12–15} Treating dielectric surfaces with self-assembled monolayers (SAMs) is one common approach and has been widely utilized for the modification of metal or oxide surfaces. In general, the reaction between SAMs and insulator surface is the driving force for self-assembly. In the case of SiO₂ or Al₂O₃, SAMs with functional groups are able to connect with the Si–OH on

dielectric surfaces and then form strong Si–O–Si bonds via elimination of hydroxyl groups. OFETs with SAMs modification exhibit a significant improvement of device performances in terms of reducing the off current, minimizing interface trap state densities, enhancing charge mobilities, and improving the current stability.^{16–23} On the other hand, solution-processed polymer dielectrics and semiconductor layers are much more attractive due to their simple fabrication process, low temperature processability (spin-coating, drop-casting or printing), and printable technique compatibility.^{24–29} However, unlike inorganic insulators, the number of reaction sites (hydroxyl groups) on polymeric dielectric surfaces are usually insufficient or even nonexistent and cannot supply appropriate chemical reactions between SAMs and dielectric surfaces. The most commonly used method for SAMs modification on polymeric dielectric surfaces is through vapor deposition of SAMs. In such conditions, the connection between interfaces

Received: June 17, 2015

Accepted: October 6, 2015

Published: October 6, 2015

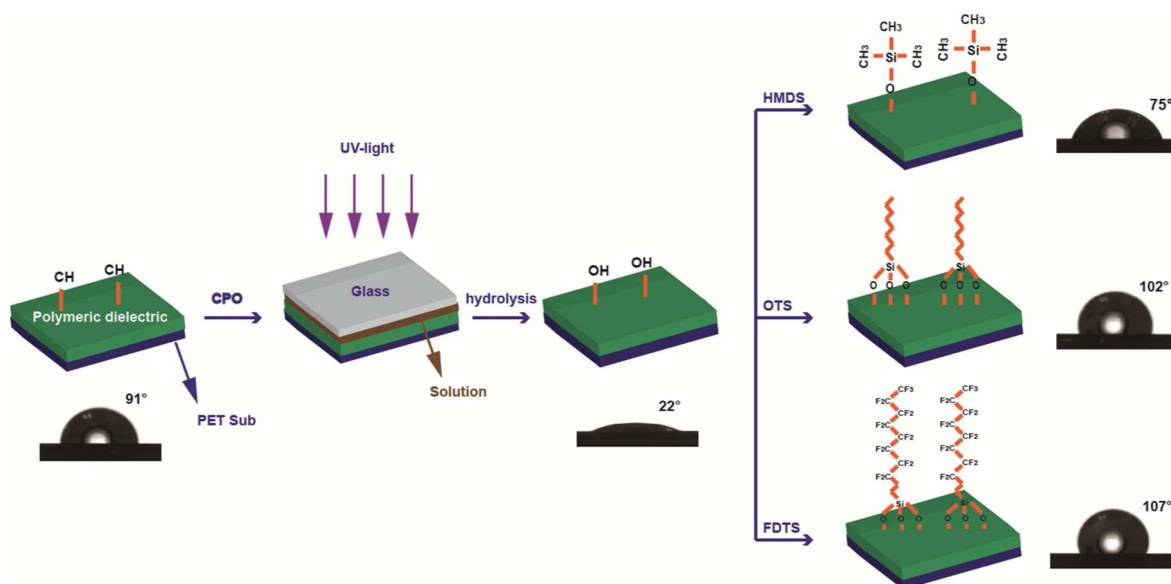


Figure 1. Schematic diagram depicting the hydroxylation and SAMs modification processes on polymeric dielectric surfaces with three different SAMs.

relies on the physical adsorption rather than tight chemical bonding.^{30,31} For the physical adsorption, the arrangement of molecules may be nonuniform and even discontinuous over a large area. Even worse, the situation becomes complicated as SAMs beneath are readily destroyed when depositing the polymer active layer via spin-coating, drop-casting, or printing. Therefore, a systematic investigation of constricted SAMs decoration on various polymeric insulators is extremely useful. The critical step of SAMs treatment on polymer surfaces is hydroxylation which provides rich reaction groups for the subsequent SAMs attachment via chemical bonding. Therefore, a delicate selection of surface treatment technique with the following requirements is necessary because very thin polymer layers are readily broken down: (i) Commonly used destroyable chemical or physical approaches such as corrosive reaction solution, UV photooxidation, and plasma treatment should be circumvented.^{32–34} (ii) The undesired oxidized products on polymer surfaces which would influence the follow-up SAMs bonding should be avoided. (iii) The hydroxylated polymer interface should be kept flat, and the bulk region of dielectric layer should be well protected. Therefore, traditional surface hydroxylation approaches coupled with the use of various high cost transition metals as catalysts or the assist with UV photooxidation or plasma treatment are not suitable for the surface treatment of polymer films. Herein, we first demonstrate the polymeric dielectric surface hydroxylation for OFETs by employing a photochemical reaction based on confined photocatalytic oxidation (CPO) treatment. The CPO technique has been applied for micropatterning of various polymer substrates.^{35–38} The principle of CPO treatment is to convert C–H bonds on the polymer surfaces to C–OSO₃[−] groups and eventually to C–OH groups by simple hydrolysis. In the CPO process, the SO₄^{•−} groups from persulfate salt is rapidly generated under the exposure of UV irradiation and alters the C–H bonds on polymer surfaces, finally leading to the formation of C–OSO₃[−] groups. By immersing the samples in ultrapure water, a surface with more stable C–OH groups is formed.³⁵ Here, we first employ this formulation for polymeric dielectric surface hydroxylation and subsequent SAMs mod-

ification in OFETs. The surface hydroxylation of three commonly used polymer insulator films of poly-4-vinylphenol (PVP), poly(methyl methacrylate) (PMMA), and polystyrene (PS) polymeric substrates have been realized. The surface topographies of modified polymeric dielectric films display a negligible roughness and undamaged polymer interface and bulk regions compared with untreated polymeric dielectric surfaces. In addition, the low leakage current of capacitors fabricated using the modified insulator films via hydroxylation shows a stable insulating property. The CPO based surface hydroxylation has been demonstrated to be applicable for various polymeric dielectric materials in OFETs. The room temperature process is compatible with the large-area and low temperature solution-processing fabrication of OFETs.

After forming rich C–OH groups as effective reaction sites on polymeric dielectric surfaces, these commonly used SAMs such as hexamethyldisilazane (HMDS), trichloro(octyl)silane (OTS), and trichloro(1H,1H,2H,2H-perfluorodecyl)silane (FDTS) are able to form a uniform monolayer on the top surface of polymer dielectric films. In this work, the n-type polymer poly{[N,N'-bis(2-octyldodecyl)naphthalene-1,4,5,8-bis(dicarboximide)-2,6-diyl]-alt-5,5'-(2,2'-bithiophene)} (P(NDI2OD-T2)) and p-type polymer poly(3-hexylthiophene) (P3HT) were utilized as semiconductor materials. For both n-type and p-type unipolar OFETs, an enhancement in mobility values has been achieved because of the surface decoration with functional groups. The ambipolar OFETs fabricated with the blend of P(NDI2OD-T2) and P3HT also exhibit enhanced and balanced mobilities with OTS decoration on polymeric dielectric surfaces. In addition, by implementing an oleophobic and hydrophobic decoration with functional FDTS, the surface roughness variation of dielectric layers by solvent corrosion was effectively reduced or even avoided when spin-coating P3HT on the top using various solvents with different boiling points, indicating the solvent resistance of polymer dielectrics is greatly improved. The proposed novel surface SAMs modification on polymeric dielectric layers would offer new opportunities for achieving organic electronics with desirable characteristics and performances.

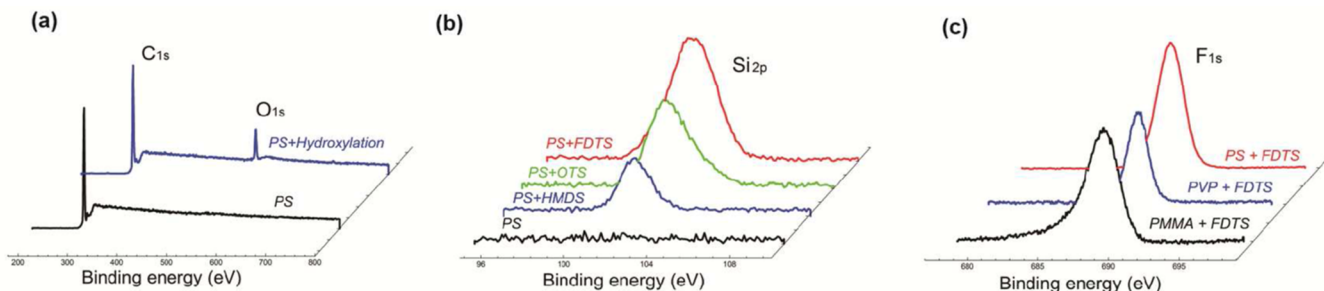


Figure 2. XPS spectra of modified and pristine PS surfaces: C_{1s} and O_{1s} peaks (a), Si_{2p} peak (b), and XPS spectra of FDTS modified PS, PVP, and PMMA surfaces, F_{1s} peak (c).

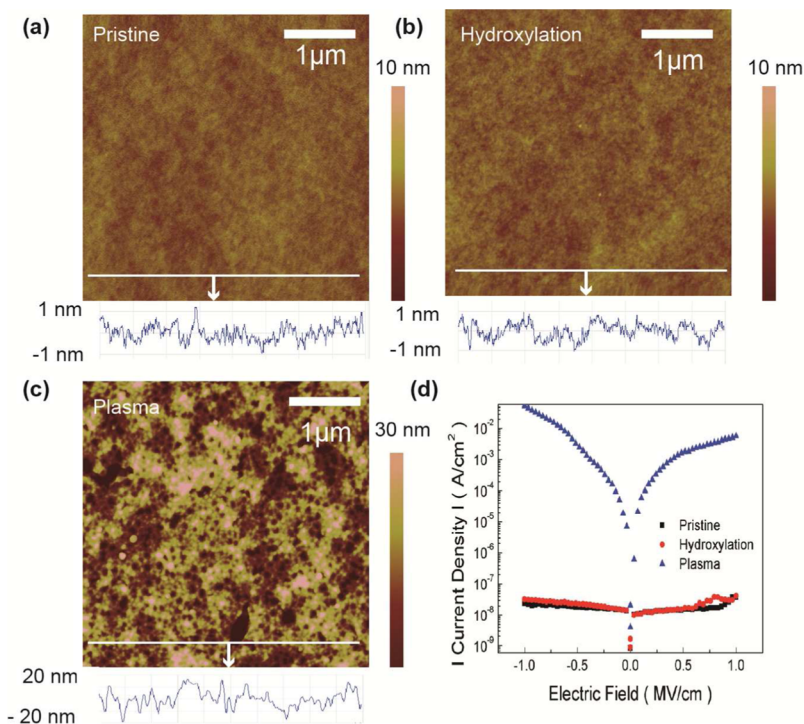


Figure 3. RMS roughness of (a) the pristine PMMA, (b) PMMA after confined photocatalytic oxidation based surface hydroxylation, and (c) PMMA with a 10 min O_2 plasma treatment. (d) Current density as a function of applied electric field of insulators with pristine PMMA, PMMA treated with CPO based hydroxylation, and O_2 plasma (10 min).

RESULTS AND DISCUSSION

Polymeric Surface Hydroxylation and SAMs Modification. The SAMs decoration process of polymeric dielectric surfaces is described in Figure 1. After depositing a polymer film on the flexible PET substrate, the CPO treatment was employed on various polymer film surfaces, followed by a hydrolysis process in ultrapure water to form rich hydroxyl groups on the top. Subsequently, three types of commonly used SAMs, HMDS, OTS, and FDTS monolayers, were successfully implanted on the treated polymeric surfaces, respectively. The surface wettability changes were monitored by contact angle variations. The interfacial chemical elements were recorded by the X-ray photoelectron spectroscopy measurement. Polystyrene (PS) was chosen here to illustrate due to the simple element composition (C and H only). As shown in Figure 1, the contact angle of PS surface reduces from 91° to 22° after surface hydroxylation. After SAMs modifications, the contact angle increases to 75° , 102° , and 107° for HMDS, OTS, and FDTS treatments, respectively. The contact angles of various SAMs surfaces are in agreement with the reported results of

SAMs decoration on SiO_2 .^{39–41} Contact angles of PS, PVP, and PMMA with various SAMs treatments are given in Table S1 (Supporting Information).

The XPS spectra of the PS sample are shown in Figure 2. Compared with the pristine PS film, the sample after hydroxylation shows a new peak O_{1s} at 532 eV in Figure 2a that cannot be observed in the pristine PS sample. The preceding results imply that OH groups have been successfully implanted onto the PS outmost surface, leading to a hydrophilic surface (22° in contact angle) as shown in Figure 1. The XPS spectra of PS samples after SAMs modification are given in Figure 2b. New peaks at around 102 eV (Si_{2p}) are observed in HMDS, OTS, and FDTS treated PS samples that are attributed to the $SiCl_3$ groups of OTS and FDTS molecules and $SiCH_3$ groups in the HMDS molecule, respectively. The XPS spectra of modified and pristine PVP and PMMA surfaces are given in Figure S1 (Supporting Information). Figure 2c demonstrates the XPS spectra of the commonly used polymers PS, PVP, and PMMA with FDTS decoration. The F_{1s} peak at around 688.5 eV is observed in all treated samples, indicating that the FDTS

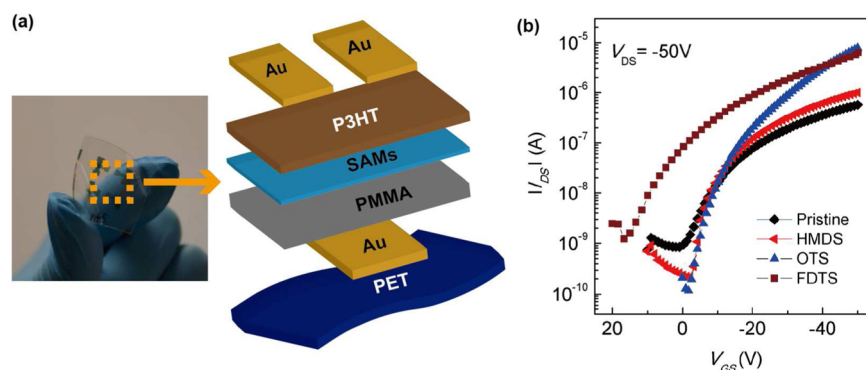


Figure 4. (a) Photograph of a 200 μm thick PET plastic sheet that consists of an array of transistors and the structure of P3HT based top-contact bottom-gate flexible OFETs with SAMs modification. (b) Transfer characteristics of P3HT based OFETs with various surface modifications on the PMMA dielectric ($V_{\text{DS}} = -50$ V).

is successfully implanted. It also reflects that the CPO based surface hydroxylation is suitable for various polymeric dielectric materials. Note that all samples were cleaned by hexane several times after surface modification. The links between the SAMs and polymeric surfaces should be the chemical bonding, rather than simple physical absorption. Otherwise, the SAMs will be easily washed away from polymer surfaces during the cleaning process.

The polymer interface morphology and insulator property after hydroxylation have been studied as shown in Figure 3. Parts a–c of Figure 3 show the variation in root-mean-square (RMS) roughness of the pristine PMMA, PMMA film after surface hydroxylation modification, and PMMA film with a 10 min O_2 plasma treatment. The O_2 plasma treatment is the reference here as it is a common approach for polymer surface modification and hydroxylation. From the AFM images, we can see that the RMS roughness of PMMA interface increases from 0.31 ± 0.03 to 0.36 ± 0.04 nm after the CPO based surface hydroxylation, indicating no significant surface roughness changes. However, the RMS roughness increases to around 5 nm after a short duration of O_2 plasma that can be seen from the cross-section images at the bottom. The current density as a function of applied electric field for 300 nm thick PMMA insulators with different treatments is given in Figure 3d. The insulating property of PMMA is significantly affected by the O_2 plasma treatment while the sample with CPO based surface hydroxylation shows a stable insulator property. During the semiconductor deposition process, a flattened dielectric interface is crucial to achieve a high quality active layer on its top surface and consequently good electrical characteristics in devices. The CPO based surface hydroxylation method demonstrates a negligible etching effect and avoids damages to the insulator property, which meets requirements for polymeric dielectric surfaces.

Unipolar OFETs and Balanced Transport in the Ambipolar OFETs. Figure 4a shows the P3HT based top-contact bottom-gate flexible OFETs structure with SAMs decoration. PET is used as the flexible substrate, and gold films are utilized as electrodes. The photograph of a 200 μm thick PET plastic sheet that consists of an array of transistors is depicted here. Transfer characteristics of P3HT based OFETs with various surface modifications on the PMMA dielectric layer are shown in Figure 4b. Here, xylene is employed to dissolve P3HT to avoid the solvent effect on the PMMA film. The devices with bare PMMA (pristine) show hole mobilities of $1.7 \pm 0.7 \times 10^{-3} \text{ cm}^2/(\text{V s})$ and an on/off ratio of 10^3 .

Meanwhile, the transistors with SAMs treatment exhibit an enhanced performance especially for those devices with OTS decoration, showing hole mobilities of $4.1 \pm 0.9 \times 10^{-2} \text{ cm}^2/(\text{V s})$ and a high on/off ratio of 10^5 . For the HMDS and FDTs modified transistors, hole mobilities are $9.3 \pm 3.1 \times 10^{-3}$ and $7.6 \pm 2.7 \times 10^{-3} \text{ cm}^2/(\text{V s})$, respectively.

Ambipolar OFETs with high balanced transport are attractive, which can be applied in the fields of light-emitting FETs and complementary-like logic circuits.^{42–44} However, usually OFETs show only electron or hole charge transport, which is attributed to the specific molecular energy levels and material structures. Here, the SAMs decoration on the polymeric dielectric is profitable to balance electron and hole transports in the ambipolar OFETs. The P(NDI2OD-T2) have been reported as a high mobility electron-transporting polymer.^{45,46} Here, by utilizing the blend of high mobility P3HT and P(NDI2OD-T2) as the semiconductor layer, the ambipolar OFETs are fabricated and the structure is depicted in Figure 5a. The schematic energy level diagram for gold metal electrodes and polymer semiconductors is shown in Figure 5b.

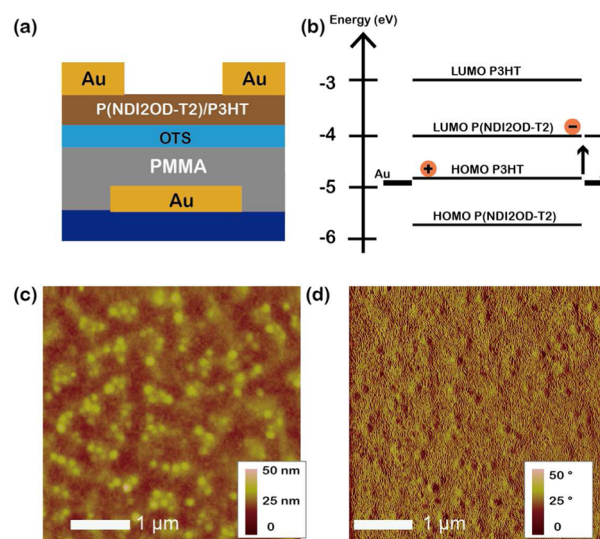


Figure 5. (a) Structure of OTS treated ambipolar OFETs. (b) Schematic energy level diagram for gold metal electrodes and polymer semiconductors. Topography (c) and phase (d) images of the P(NDI2OD-T2) and P3HT blend on the OTS treated PMMA surface.

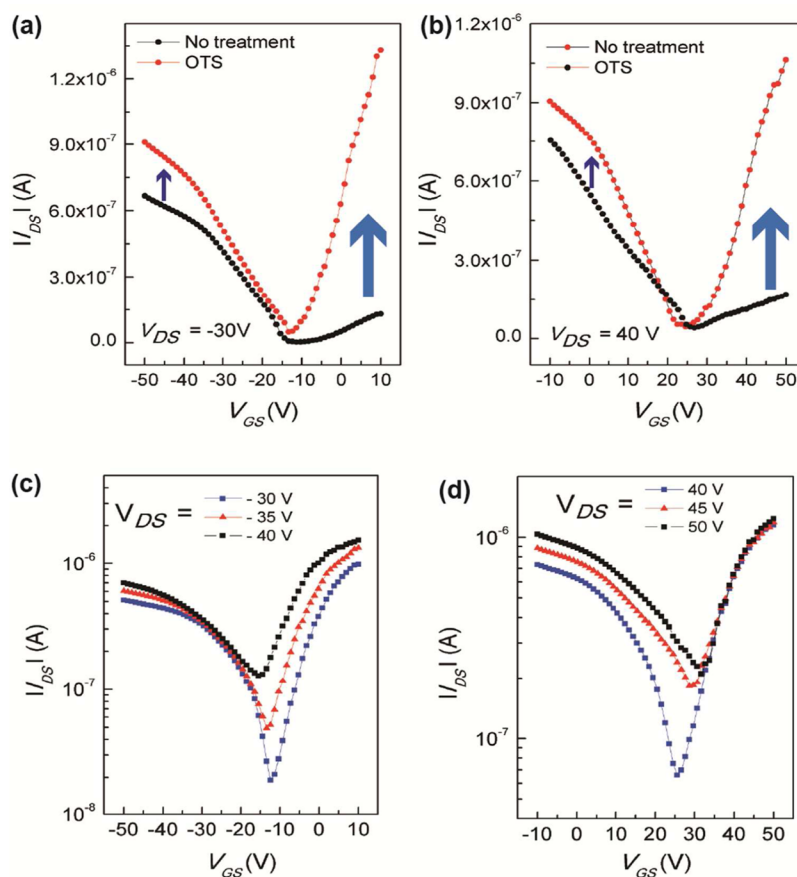


Figure 6. Transfer characteristics of the ambipolar polymer blend FETs modified with and without OTS monolayers: (a) p-type operation mode ($V_{DS} = -30$ V) and (b) n-type operation mode ($V_{DS} = 40$ V). Typical transfer characteristics of the OTS modified ambipolar polymer blend FETs in (c) p-type operation mode and (d) n-type operation mode in different drain biases.

Obviously, the hole injection barrier between the P3HT HOMO level and the work function of electrodes is small (0.1 eV), while the electron injection barrier is about 0.9 eV.

Transfer characteristics of ambipolar OFETs based on the polymer heterojunction semiconductor blend are shown in Figure 6. For the device with the OTS treated polymeric dielectric surface, the transfer curve shows a balanced transport under both positive and negative drain biases with electron saturation mobilities of $5.7 \pm 2.9 \times 10^{-3}$ $\text{cm}^2/(\text{V s})$ at $V_{DS} = 40$ V and hole saturation mobilities of $3.1 \pm 1.2 \times 10^{-3}$ $\text{cm}^2/(\text{V s})$ at $V_{DS} = -40$ V. The significant increase in the mobility especially for the electron due to the OTS surface modification achieves the formation of balanced transport. The influence of OTS on the performance of unipolar n-type transistors is given in Figure S2 (Supporting Information). The electron mobilities enhance from $3.1 \pm 1.2 \times 10^{-3}$ to $1.8 \pm 0.8 \times 10^{-1}$ $\text{cm}^2/(\text{V s})$. In the ambipolar OFETs, the threshold voltages V_{TH} for n-channel operation are +26 and -6 V for p-channel operation. The high threshold voltage in the positive bias region is probably caused by the relatively high charge injection barrier, as shown in Figure 5b. The surface topography and phase of the polymer heterojunction film were characterized by AFM as shown in Figure 5c,d. The surface of the blend film is smooth with RMS roughness 2.9 ± 0.7 nm. Note that mobilities in the ambipolar OFETs are not obviously smaller than the mobility value in the unipolar devices; it is probably indicative that the existence of a polymer network acts as a pathway for both electron and hole carriers transport.

Solvent Effects on Polymeric Gate Dielectrics. In OFETs with polymeric gate dielectrics, the solvent effect limits the choice on materials for both dielectrics and semiconductors. Therefore, finding an appropriate way to preclude the solvent effect is essential. Here, the FDS treatment is employed to preclude the solvent effect. By successful targeted functionalization, the interface properties of polymeric gate dielectrics are improved. The P3HT transistors with SiO_2 as insulator by spin-coating using various solvents with different boiling points have been demonstrated by Chang et al.⁴⁷ The authors found an enhancement in the mobility by using high-boiling-point solvents compared with low-boiling-point ones, since rapid evaporation limits the time for crystallization of P3HT during spin-coating. However, the condition would be complicated when the insulator layer is a polymeric dielectric film as the solvent effect should also be considered. The solvent for dissolving semiconductor polymer could possibly dissolve the polymeric dielectric layer underneath. The surface roughness can be enlarged which is related to the solubility parameter and finally influences the active layer quality and the subsequent device performance.⁴⁸ Therefore, for a specific polymeric dielectric layer, the solvent effect limits the choice of solvents and further influences the improvement of the active layer quality. On the other hand, the polymer semiconductor material that can only form a good solution in a specific solvent also limits the choice of polymeric dielectric layer at the bottom. Here, the solvent effect in OFETs based on the polymeric dielectric layer is investigated. The results show that

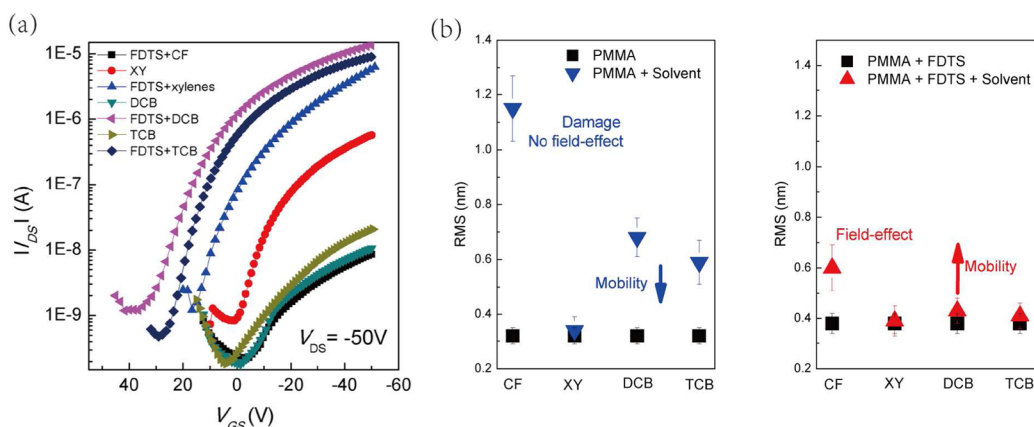


Figure 7. (a) Transfer characteristics of the P3HT based OFETs with spin-coating P3HT using various solvents ($V_{DS} = -50$ V). (b) RMS changes of the pristine PMMA and FDTs modified PMMA dielectrics with various solvent treatments. Average values with error bars (using standard deviation) are given for 10 different devices for each type of dielectric layers.

the FDTs modification is utilized to relieve or even avoid the influence of solvent effects. Here, PMMA is utilized as the dielectric layer. The electrical properties of devices based on spin-coated P3HT using various solvents including xylenes (XY-P3HT), chloroform (CF-P3HT), dichlorobenzene (DCB-P3HT), and 1,2,4-trichlorobenzene (TCB-P3HT) are measured. The transfer characteristics of OFETs with spin-coated P3HT as semiconductor layer using various solvents are shown in Figure 7a. The XY-P3HT transistors show the highest mobilities of $1.6 \pm 0.8 \times 10^{-3} \text{ cm}^2/(\text{V s})$. However, the DCB-P3HT and TCB-P3HT transistors show a worse performance with mobilities of $9.7 \pm 3.6 \times 10^{-5}$ and $2.2 \pm 0.8 \times 10^{-4} \text{ cm}^2/(\text{V s})$. For the CF-P3HT devices, no field effect is observed as the PMMA film is completely destroyed during the P3HT spin-coating process. The FDTs modification has been carried out on the PMMA film surface, and the device performance exhibits an obvious improvement especially for the DCB-P3HT and TCB-P3HT devices. The mobilities of $8.6 \pm 2.9 \times 10^{-3}$ and $1.5 \pm 0.8 \times 10^{-2} \text{ cm}^2/(\text{V s})$, 2 orders of magnitude larger than the devices without treatment, are observed. At the same time, as shown in Figure 7a, after the FDTs modification, the CF-P3HT transistors show the field effect, with hole mobilities of $2.1 \pm 0.9 \times 10^{-4} \text{ cm}^2/(\text{V s})$. The RMS roughness changes of PMMA and FDTs modified PMMA dielectric surfaces with various solvent treatments are given in Figure 7b. Here, various organic solvents (without P3HT) are spin-coated on the top of polymeric films. For the PMMA samples with various solvents spin-coated on the top, the solvent effect dramatically increases the surface roughness except for xylenes, leading to an inferior device performance. However, the spin-coating on the surface of an oleophobic and hydrophobic protective FDTs layer effectively reduces or even avoids the solvents induced roughness increase. For the chloroform treatment, due to the FDTs layer on the top, the RMS roughness reduced from 1.15 ± 0.2 to 0.60 ± 0.1 nm in comparison with the PMMA film without treatment and the field effect is observed in the device measurement. For the DCB and TCB solvents, RMS roughness values of 0.43 ± 0.05 and 0.41 ± 0.04 nm are obtained, almost a negligible change in comparison with the FDTs modified PMMA layer (around 0.37 nm). Note that the protection of the FDTs layer for solvents is only applicable for the short time spin-coating process. The boiling points of chloroform, xylenes, DCB, and TCB are 61, 138, 179, and 219 °C, respectively. From all of the preceding details, we can find out that the

solvent effect dominates the device performance when there is no protective layer on the top. However, when the solvent effect has been avoided for the DCB-P3HT and TCB-P3HT devices with FDTs modification, the high-boiling-point solvent contributes to an enhanced mobility because the low evaporation time produces a better active layer.

CONCLUSION

Surface hydroxylation on a series of polymeric dielectric surfaces based on the CPO approach has been successfully demonstrated and applied for OFETs' interface modification. The method exhibits a negligible etching effect and offers an undestroyed insulator property for polymeric dielectric layers. The flexible OFETs based on various types of SAMs modification via chemical bonding exhibit an obvious improvement in the device performance. In comparison with untreated devices, 2 orders of magnitude enhancement of the charge carrier mobility is observed for surface treated transistors. Meanwhile, a balanced and enhanced mobility has been obtained after surface modification on the PMMA dielectric surface. Furthermore, the solvent effect can be reduced or even avoided with the oleophobic and hydrophobic FDTs modification on the polymeric dielectric layer. The proposed novel surface SAMs modification offers new opportunities for targeted surface functionalization for organic electronic devices.

METHODS

Materials. Commercially available 200 μm thick PET was utilized as the flexible substrate. Material ammonium persulfate (APS), hexamethyldisilazane ($(\text{CH}_3)_3\text{SiNHSi}(\text{CH}_3)_3$, HMDS), trichloro(octyl)silane ($\text{CH}_3(\text{CH}_2)_7\text{SiCl}_3$, OTS), trichloro(1H,1H,2H,2H-perfluorodecyl)silane ($\text{CF}_3(\text{CF}_2)_7(\text{CH}_2)_2\text{-SiCl}_3$, FDTs), poly-4-vinyl-phenol (PVP, $M_w = 25000$ g/mol), poly(methyl methacrylate) (PMMA, $M_w = 120000$ g/mol), and poly(3-hexylthiophene-2,5-diyl) (P3HT, average $M_n = 54000\text{--}75000$) were commercially available from Aldrich. Polystyrene (PS, $M_w = 2000000$ g/mol) was purchased from Alfa. The n-type polymer (NDI) naphthalenebis(dicarboximide) based P(NDI2OD-T2) was available from Polyera Corp. All materials including solvents hexane, chloroform, xylenes, 1,4-dichlorobenzene (DCB), 1,2,4-trichlorobenzene (TCB), and propylene glycol mono-methyl ether acetate (PGMEA) were utilized without further purification.

Device Fabrication and Characterization. Bottom-gate/top-contact all polymer OFETs were fabricated on PET substrates. After being cleaned by deionized water first, a 100 nm thick gold film was

thermally evaporated on the PET surface through a patterned mask as the gate electrode. Then, PMMA (50 mg mL⁻¹), PVP (50 mg mL⁻¹), or PS (30 mg mL⁻¹) solutions, dissolved in toluene, PGMEA, and chlorobenzene solvents, were deposited on flexible surfaces with a speed of 2000 rpm for 40 s, followed by an annealing process at 120 °C for 30 min on a hot plate in the Mbraun nitrogen glovebox. All solutions were filtered through a 0.2 μm syringe filter before being used. After then, the persulfate salt aqueous solution (30 wt %) was coated on surfaces of the polymeric dielectric films, followed by covering with a quartz glass to form a sandwich structure with a very thin liquid layer (around 2 μm) in the middle. Then, the structure was irradiated under UV light from the topside for 15 min. After then, with a simple cleaning step with ultrapure water, substrates were immersed into ultrapure water for conducting hydrolysis to form a stable surface full of C–OH groups. For the process of SAMs modification on polymeric surfaces, the HMDS modification was performed through deposition of HMDS vapor in a chamber. For the OTS and FOTS SAMs modification, the polymer substrates full of OH groups were immersed in the OTS or FOTS hexane solution (0.1 wt %). Then, substrates were cleaned to remove unreacted and physisorbed silanes and then placed on a hot plate at 130 °C for 30 min to form an ordered SAMs arrangement. During the semiconductor film fabrication process, the polymer P3HT dissolved in xylenes, chloroform, DCB, or TCB (5 mg mL⁻¹), and the ambipolar active layer, the semiconductor blend of P3HT and P(NDI2OD-T2) (in the proportion of 1:1 by weight) from a xylenes solution, were spun at 1000 rpm for 1 min on polymeric dielectric layers, followed by a postannealing process at 120 °C for 40 min. All of the film fabrication processes were operated in the Mbraun nitrogen glovebox to avoid contamination from oxygen and water. Subsequently, a gold film (100 nm) was vacuum sublimed on the active layer through a shadow mask ($L/W = 50 \mu\text{m}/1000 \mu\text{m}$) with a speed of 0.2 Å/s to form source/drain electrodes. The surface topographies of polymeric dielectric surface were measured by AFM (VEECO Multimode V, tapping mode). The contact angles were measured by a Ramehart Model 250-F1 standard goniometer with DROP image Advanced 2.1. XPS was scanned by a Physical Electronics PHI 5802 instrument with a monochromatic Al K α X-ray source in the ultrahigh vacuum condition. All I – V characterizations of devices were performed using a Keithley 6212 source meter, Agilent 4155C semiconductor parameter analyzer, and HP 4284A LCR meter in a MBraun nitrogen glovebox. Average values with error bars (using standard deviation) bars were given after characterizing 10 distinct devices for each type of dielectric layers.

■ ASSOCIATED CONTENT

● Supporting Information

The Supporting Information is available free of charge on the ACS Publications website at DOI: 10.1021/acsami.5b05363.

XPS spectra and table of contact angles of PVP and PMMA surfaces and transfer characteristics of the n-type OFETs based on P(NDI2OD-T2) modified with and without OTS monolayers (PDF)

■ AUTHOR INFORMATION

Corresponding Author

*E-mail: val.roy@cityu.edu.hk.

Notes

The authors declare no competing financial interest.

■ ACKNOWLEDGMENTS

We acknowledge funding from City University of Hong Kong's Research Grant Project No. 7004378.

■ REFERENCES

- (1) Liu, S.; Wang, W. M.; Briseno, A. L.; Mannsfeld, S. C. B.; Bao, Z. Controlled Deposition of Crystalline Organic Semiconductors for Field-Effect-Transistor Applications. *Adv. Mater.* **2009**, *21*, 1217–1232.
- (2) Liu, C.; Jang, J.; Xu, Y.; Kim, H.-J.; Khim, D.; Park, W.-T.; Noh, Y.-Y.; Kim, J.-J. Effect of Doping Concentration on Microstructure of Conjugated Polymers and Characteristics in N-Type Polymer Field-Effect Transistors. *Adv. Funct. Mater.* **2015**, *25*, 758–767.
- (3) Zaumseil, J.; Sirringhaus, H. Electron and Ambipolar Transport in Organic Field-Effect Transistors. *Chem. Rev.* **2007**, *107*, 1296–1323.
- (4) Wen, Y.; Liu, Y.; Guo, Y.; Yu, G.; Hu, W. Experimental Techniques for the Fabrication and Characterization of Organic Thin Films for Field-Effect Transistors. *Chem. Rev.* **2011**, *111*, 3358–406.
- (5) Moonen, P. F.; Yakimets, I.; Huskens, J. Fabrication of Transistors on Flexible Substrates: from Mass-Printing to High-Resolution Alternative Lithography Strategies. *Adv. Mater.* **2012**, *24*, 5526–5541.
- (6) Guo, Y.; Yu, G.; Liu, Y. Functional Organic Field-Effect Transistors. *Adv. Mater.* **2010**, *22*, 4427–4447.
- (7) Braga, D.; Horowitz, G. High-Performance Organic Field-Effect Transistors. *Adv. Mater.* **2009**, *21*, 1473–1486.
- (8) Hwang, S.-W.; Kim, D.-H.; Tao, H.; Kim, T.-i.; Kim, S.; Yu, K. J.; Panilaitis, B.; Jeong, J.-W.; Song, J.-K.; Omenetto, F. G.; Rogers, J. A. Materials and Fabrication Processes for Transient and Bioresorbable High-Performance Electronics. *Adv. Funct. Mater.* **2013**, *23*, 4087–4093.
- (9) Dimitrakopoulos, C. D.; Malenfant, P. R. L. Organic Thin Film Transistors for Large Area Electronics. *Adv. Mater.* **2002**, *14*, 99–117.
- (10) Yan, Y.; She, X. J.; Zhu, H.; Wang, S. D. Origin of Bias Stress Induced Instability of Contact Resistance in Organic Thin Film Transistors. *Org. Electron.* **2011**, *12*, 823–826.
- (11) Wang, S. D.; Yan, Y.; Tsukagoshi, K. Transition-Voltage Method for Estimating Contact Resistance in Organic Thin-Film Transistors. *IEEE Electron Device Lett.* **2010**, *31*, 509–511.
- (12) Scheinert, S.; Pernstich, K. P.; Batlogg, B.; Paasch, G. Determination of Trap Distributions from Current Characteristics of Pentacene Field-Effect Transistors with Surface Modified Gate Oxide. *J. Appl. Phys.* **2007**, *102*, 104503.
- (13) Chou, W.-Y.; Kuo, C.-W.; Cheng, H.-L.; Chen, Y.-R.; Tang, F.-C.; Yang, F.-Y.; Shu, D.-Y.; Liao, C.-C. Effect of Surface Free Energy in Gate Dielectric in Pentacene Thin-film Transistors. *Appl. Phys. Lett.* **2006**, *89*, 112126.
- (14) Kelley, T. W.; Boardman, L. D.; Dunbar, T. D.; Muryes, D. V.; Pellerite, M. J.; Smith, T. P. High-Performance OTFTs Using Surface-Modified Alumina Dielectrics. *J. Phys. Chem. B* **2003**, *107*, 5877–5881.
- (15) Kim, J.-M.; Lee, J.-W.; Kim, J.-K.; Ju, B.-K.; Kim, J.-S.; Lee, Y.-H.; Oh, M.-H. An Organic Thin-film Transistor of High Mobility by Dielectric Surface Modification with Organic Molecule. *Appl. Phys. Lett.* **2004**, *85*, 6368.
- (16) Kobayashi, S.; Nishikawa, T.; Takenobu, T.; Mori, S.; Shimoda, T.; Mitani, T.; Shimotani, H.; Yoshimoto, N.; Ogawa, S.; Iwasa, Y. Control of Carrier Density by Self-Assembled Monolayers in Organic Field-Effect Transistors. *Nat. Mater.* **2004**, *3*, 317–22.
- (17) Wang, S. D.; Miyadera, T.; Minari, T.; Aoyagi, Y.; Tsukagoshi, K. Correlation between Grain Size and Device Parameters in Pentacene Thin Film Transistors. *Appl. Phys. Lett.* **2008**, *93*, 043311.
- (18) Takeya, J.; Nishikawa, T.; Takenobu, T.; Kobayashi, S.; Iwasa, Y.; Mitani, T.; Goldmann, C.; Krellner, C.; Batlogg, B. Effects of Polarized Organosilane Self-Assembled Monolayers on Organic Single-Crystal Field-Effect Transistors. *Appl. Phys. Lett.* **2004**, *85*, 5078.
- (19) Youn, J.; Dholakia, G. R.; Huang, H.; Hennek, J. W.; Facchetti, A.; Marks, T. J. Influence of Thiol Self-Assembled Monolayer Processing on Bottom-Contact Thin-Film Transistors Based on N-Type Organic Semiconductors. *Adv. Funct. Mater.* **2012**, *22*, 1856–1869.
- (20) DiBenedetto, S. A.; Facchetti, A.; Ratner, M. A.; Marks, T. J. Molecular Self-Assembled Monolayers and Multilayers for Organic and Unconventional Inorganic Thin-Film Transistor Applications. *Adv. Mater.* **2009**, *21*, 1407–1433.

- (21) Shao, W.; Dong, H.; Jiang, L.; Hu, W. Morphology Control for High Performance Organic Thin Film Transistors. *Chem. Sci.* **2011**, *2*, 590–600.
- (22) Knipp, D.; Street, R. A.; Völkel, A.; Ho, J. Pentacene Thin Film Transistors on Inorganic Dielectrics: Morphology, Structural Properties, and Electronic Transport. *J. Appl. Phys.* **2003**, *93*, 347–355.
- (23) Salleo, A.; Chabinyc, M. L.; Yang, M. S.; Street, R. A. Polymer Thin-Film Transistors with Chemically Modified Dielectric Interfaces. *Appl. Phys. Lett.* **2002**, *81*, 4383.
- (24) Wang, J. Z.; Zheng, Z. H.; Li, H. W.; Huck, W. T.; Sirringhaus, H. Dewetting of Conducting Polymer Inkjet Droplets on Patterned Surfaces. *Nat. Mater.* **2004**, *3*, 171–6.
- (25) Sirringhaus, H.; Kawase, T.; Friend, R. H.; Shimoda, T.; Inbasekaran, M.; Wu, W.; Woo, E. P. High-Resolution Inkjet Printing of All-Polymer Transistor Circuits. *Science* **2000**, *290*, 2123–2126.
- (26) Sun, J.; Zhang, B.; Katz, H. E. Materials for Printable, Transparent, and Low-Voltage Transistors. *Adv. Funct. Mater.* **2011**, *21*, 29–45.
- (27) Katz, H. E. Recent Advances in Semiconductor Performance and Printing Processes for Organic Transistor-Based Electronics. *Chem. Mater.* **2004**, *16*, 4748–4756.
- (28) Zhang, L.; Di, C.-a.; Yu, G.; Liu, Y. Solution Processed Organic Field-Effect Transistors and Their Application in Printed Logic Circuits. *J. Mater. Chem.* **2010**, *20*, 7059.
- (29) Smith, J.; Hamilton, R.; McCulloch, I.; Stingelin-Stutzmann, N.; Heeney, M.; Bradley, D. D. C.; Anthopoulos, T. D. Solution-Processed Organic Transistors Based on Semiconducting Blends. *J. Mater. Chem.* **2010**, *20*, 2562.
- (30) Park, J.; Kim, H.; Kim, J.-H.; Lee, J. W.; Choi, J. S. Characteristics of Organic Thin-Film Transistors with Self-Assembled Monolayer Formed in Gas-Phase on PVP Gate Insulator. *Mol. Cryst. Liq. Cryst.* **2009**, *505*, 97–103.
- (31) Yang, F.-Y.; Chang, K.-J.; Hsu, M.-Y.; Liu, C.-C. High-Performance Poly(3-hexylthiophene) Transistors with Thermally Cured and Photo-cured PVP Gate Dielectrics. *J. Mater. Chem.* **2008**, *18*, 5927–5932.
- (32) Lee, J. H.; Park, J. W.; Lee, H. B. Cell Adhesion and Growth on Polymer Surfaces with Hydroxyl Groups Prepared by Water Vapour Plasma Treatment. *Biomaterials* **1991**, *12*, 443–448.
- (33) Murakami, T. N.; Fukushima, Y.; Hirano, Y.; Tokuoka, Y.; Takahashi, M.; Kawashima, N. Modification of PS Films by Combined Treatment of Ozone Aeration and UV Irradiation in Aqueous Ammonia Solution for the Introduction of Amine and Amide Groups on Their Surface. *Appl. Surf. Sci.* **2005**, *249*, 425–432.
- (34) Ferguson, G. S.; Chaudhury, M. K.; Biebuyck, H. A.; Whitesides, G. M. Monolayers on Disordered Substrates: Self-Assembly of Alkyltrichlorosilanes on Surface-Modified Polyethylene and Poly(dimethylsiloxane). *Macromolecules* **1993**, *26*, 5870–5875.
- (35) Yang, P.; Yang, W. Hydroxylation of Organic Polymer Surface: Method and Application. *ACS Appl. Mater. Interfaces* **2014**, *6*, 3759–70.
- (36) Mu, X.; Guo, S.; Zhang, L.; Yang, P. Modification of Indium Tin Oxide with Persulfate-Based Photochemistry Toward Facile, Rapid, and Low-Temperature Interface-Mediated Multicomponent Assembling. *Langmuir* **2014**, *30*, 4945–51.
- (37) Yang, P.; Yang, M.; Zou, S.; Xie, J.; Yang, W. Positive and Negative TiO₂ Micropatterns on Organic Polymer Substrates. *J. Am. Chem. Soc.* **2007**, *129*, 1541–1552.
- (38) Yang, P.; Zou, S.; Yang, W. Positive and Negative ZnO Micropatterning on Functionalized Polymer Surfaces. *Small* **2008**, *4*, 1527–36.
- (39) Veres, J.; Ogier, S.; Lloyd, G.; de Leeuw, D. Gate Insulators in Organic Field-Effect Transistors. *Chem. Mater.* **2004**, *16*, 4543–4555.
- (40) Joseph Kline, R.; McGehee, M. D.; Toney, M. F. Highly Oriented Crystals at the Buried Interface in Polythiophene Thin-Film Transistors. *Nat. Mater.* **2006**, *5*, 222–228.
- (41) Janssen, D.; De Palma, R.; Verlaak, S.; Heremans, P.; Dehaen, W. Static Solvent Contact Angle Measurements, Surface Free Energy and Wettability Determination of Various Self-Assembled Monolayers on Silicon Dioxide. *Thin Solid Films* **2006**, *515*, 1433–1438.
- (42) Bürgi, L.; Turbiez, M.; Pfeiffer, R.; Bienewald, F.; Kirner, H.-J.; Winnewisser, C. High-Mobility Ambipolar Near-Infrared Light-Emitting Polymer Field-Effect Transistors. *Adv. Mater.* **2008**, *20*, 2217–2224.
- (43) Meijer, E. J.; de Leeuw, D. M.; Setayesh, S.; van Veenendaal, E.; Huisman, B. H.; Blom, P. W. M.; Hummelen, J. C.; Scherf, U.; Klapwijk, T. M. Solution-Processed Ambipolar Organic Field-Effect Transistors and Inverters. *Nat. Mater.* **2003**, *2*, 678–682.
- (44) Yan, Y.; Sun, Q.-J.; Gao, X.; Deng, P.; Zhang, Q.; Wang, S.-D. Probing Bias Stress Effect and Contact Resistance in Bilayer Ambipolar Organic Field-Effect Transistors. *Appl. Phys. Lett.* **2013**, *103*, 073303.
- (45) Szendrei, K.; Jarzab, D.; Chen, Z.; Facchetti, A.; Loi, M. A. Ambipolar All-Polymer Bulk Heterojunction Field-Effect Transistors. *J. Mater. Chem.* **2010**, *20*, 1317.
- (46) Yan, H.; Chen, Z.; Zheng, Y.; Newman, C.; Quinn, J. R.; Dotz, F.; Kastler, M.; Facchetti, A. A High-Mobility Electron-Transporting Polymer for Printed Transistors. *Nature* **2009**, *457*, 679–86.
- (47) Chang, J.-F.; Sun, B.; Breiby, D. W.; Nielsen, M. M.; Sölling, T. I.; Giles, M.; McCulloch, I.; Sirringhaus, H. Enhanced Mobility of Poly(3-hexylthiophene) Transistors by Spin-Coating from High-Boiling-Point Solvents. *Chem. Mater.* **2004**, *16*, 4772–4776.
- (48) Park, J.; Park, S. Y.; Shim, S.-O.; Kang, H.; Lee, H. H. A Polymer Gate Dielectric for High-Mobility Polymer Thin-Film Transistors and Solvent Effects. *Appl. Phys. Lett.* **2004**, *85*, 3283.